

Software-Defined Radio LTE Positioning Receiver Towards Future Hybrid Localization Systems

José A. del Peral-Rosado*, José A. López-Salcedo, Gonzalo Seco-Granados,
Department of Telecommunications and System Engineering,
Universitat Autònoma de Barcelona (UAB), 08193 Cerdanyola del Vallès, Spain

Francesca Zanier, Paolo Crosta, Rigas Ioannides, and Massimo Crisci
Radio Navigation Systems and Techniques Section,
European Space Agency/ESTEC, 2201 AZ Noordwijk, The Netherlands

The appropriate positioning characteristics and fast deployment of Long Term Evolution (LTE) systems makes this technology a promising candidate towards future satellite and terrestrial hybrid scenario. Nevertheless, further studies on the achievable LTE positioning capabilities are still necessary for commercial or realistic network deployments. This paper describes a tool that provides standalone localization in LTE networks. The tool is a software-defined radio (SDR) receiver working at the LTE physical layer, performing acquisition, tracking and positioning. The SDR LTE positioning receiver is validated in a static scenario, showing position errors below three meters in the absence of multipath for a signal bandwidth of 1.08 MHz.

Nomenclature

3GPP	3 rd Generation Partnership Project
AWGN	Additive White Gaussian Noise
BS	Base Station
CFO	Carrier Frequency Offset
CP	Cyclic Prefix
CRS	Cell-specific Reference Signal
DLL	Delay Lock Loop
E-SMLC	Evolved Serving Mobile Location Centre
E-UTRA	Evolved Universal Terrestrial Radio Access
EARFCN	E-UTRA Absolute Radio Frequency Channel Number
FDD	Frequency Division Duplexing
FFT	Fast Fourier Transform
GNSS	Global Navigation Satellite Systems
LPP	LTE Positioning Protocol
LTE	Long Term Evolution
ML	Maximum Likelihood
NDA	Non-Data-Aided
OFDM	Orthogonal Frequency Division Multiplexing
OTDoA	Observed Time Difference Of Arrival
PBCH	Physical Broadcast CHannel
PCFICH	Physical Control Format Indicator CHannel
PDCCH	Physical Downlink Control CHannel
PDSCH	Physical Downlink Shared CHannel

*Emails: {JoseAntonio.DelPeral, Jose.Salcedo, Gonzalo.Seco}@uab.cat, {Francesca.Zanier, Paolo.Crosta, Rigas.Ioannides, Massimo.Crisci}@esa.int; Corresponding author phone: +34 93 581 3843

PHICH	Physical Hybrid-ARQ Indicator CHannel
PLL	Phase Lock Loop
PRS	Positioning Reference Signal
PSS	Primary Synchronization Signal
RB	Resource Block
RSTD	Reference Signal Time Difference
SDR	Software-Defined Radio
SF	Subframe
SFN	Single-Frequency Network
SNR	Signal-to-Noise Ratio
SSS	Secondary Synchronization Signal
TDE	Time Delay Estimation
USRP	Universal Software Radio Peripheral
UHD	USRP hardware driver

I. Introduction

The fast worldwide spreading of next-generation mobile communications, such as the Long Term Evolution (LTE), is originating new technologies and applications. LTE cellular networks not only offer higher data transmission rates with respect to their predecessors, but introduce new features to further enhance their performance. One of these features is the positioning capability, which is introduced in Release 9 of the standard by defining a dedicated downlink signal for Observed Time Difference of Arrival (OTDoA), i.e. the positioning reference signal (PRS).^{1,2} In the context of localization, Global Navigation Satellite Systems (GNSS) have led the provision of high accurate position estimates worldwide. In contrast, the use of cellular networks for positioning has been traditionally reduced to aid GNSS receivers with assistance data (i.e. Assisted-GNSS).³ Now, LTE technology may not only be used for complementing GNSS systems, but it is actually a technology capable of providing localization information by itself, using the time delay estimation (TDE) of the downlink signals. Thus, GNSS and LTE signals can be combined into a hybrid satellite and terrestrial localization system with potential to improve the nominal accuracy in harsh environments, such as urban canyons or indoor scenarios.

Until the introduction of LTE, cellular communications systems have generally not provided very accurate synchronization among base stations (BS), neither wideband signals, which are two main enabling features to obtain accurate time delay estimates. Despite the appropriate characteristics of the LTE downlink signal for positioning and the fast deployment of LTE networks,⁴ very few commercial LTE systems are already capable of locating the user by means of OTDoA positioning. According to Ref. 5, OTDoA with LTE is still an emerging technology that is not yet available for evaluation in emergency call location trials. Thus, the hybridization of LTE and GNSS signals for localization is still a challenge.

The LTE positioning performance was analysed during the standardization process produced by the 3rd Generation Partnership Project (3GPP) consortium.^{6,7} Further details were described with an specific methodology to study the LTE position accuracy.^{8,9} In addition, prototype deployments showed the OTDoA location performance in realistic environments,¹⁰ even with a hybrid LTE and GNSS solution.¹¹ However, it is still necessary to assess the achievable localisation accuracy of LTE in commercial deployments, and thus to explore the potential of hybrid satellite and terrestrial positioning solutions. In order to help on contributing to this goal, this paper describes a tool to produce time delay and position estimates in LTE networks. The tool to be presented is a software-defined radio (SDR) receiver that exploits the positioning capabilities of the LTE signals. The SDR LTE positioning receiver employs a Universal Software Radio Peripheral (USRP) platform and MATLAB to digitalize and process the signal, respectively. The receiver works at the physical layer by implementing accurate time and frequency synchronization methods for LTE signals. The time delay estimation can be performed standalone without the positioning assistance data provided by the LTE Positioning Protocol (LPP), but the precise location of the base stations is required to compute the user location. The remainder of this paper is organized as follows. Section II introduces the specification of the LTE downlink signals, focusing on the pilot signals. Section III describes the main modules of the SDR LTE positioning receiver. In Section IV, the performance of the receiver is validated with numerical results for a static scenario. Finally, conclusions are drawn in Section V.

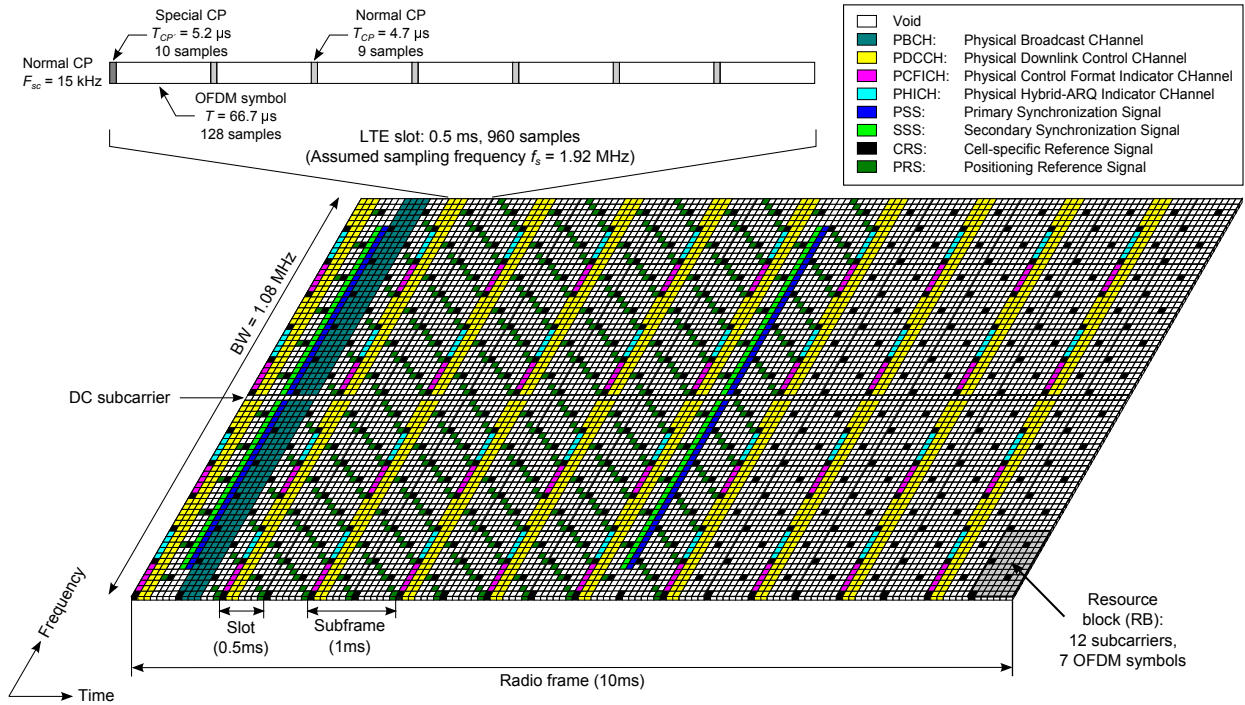


Figure 1. Time-frequency grid of the LTE signals specified in Release 9 of the standard for 6 RB, frame structure type 1 (applicable to FDD) and normal cyclic prefix (CP), assuming a sampling frequency of 1.92 MHz and unicast transmission without user data.

II. Long Term Evolution

One of the main features introduced by LTE in mobile communications is the use of multicarrier signals in the downlink transmission. The multicarrier waveform introduces flexibility, spectral efficiency and robustness against frequency-selective fading introduced by multipath, among other advantages with respect to traditional single carrier signals. Particularly, the LTE downlink transmission is based on the Orthogonal Frequency Division Multiplexing (OFDM) modulation, which is defined as

$$x_c(t) = \sqrt{\frac{C}{N}} \sum_{n=0}^{N-1} b(n) \exp\left(j \frac{2\pi n t}{T}\right), \quad 0 < t < T, \quad (1)$$

where C is the power of the band-pass signal, N is the total number of subcarriers, $b(n)$ is the complex-valued symbol transmitted at the n -th subcarrier, and T is the OFDM symbol period. According to the physical layer specification,¹ the symbol period T is equal to $66.67 \mu\text{s}$, which corresponds to a subcarrier spacing $F_{sc} = 1/T$ of 15 kHz. In order to avoid intersymbol interference (ISI), the end of the OFDM symbol is added at the beginning, forming the well-known cyclic prefix (CP). The normal CP configuration and FDD transmission will be adopted in this paper, resulting in a special CP period $T_{CP'}$ of $5.2 \mu\text{s}$ and a normal CP period T_{CP} of $4.7 \mu\text{s}$. The minimum resource allocation is called resource block (RB), and is formed by resource elements along 7 OFDM symbols and 12 subcarriers in this normal CP configuration. Thus, the transmission grid of a base station is defined in time and frequency, as it is shown in figure 1. The system bandwidth is scalable from 1.4 MHz to 20 MHz, but guard bands are left at the edges of the spectrum, thus only allowing a minimum transmission bandwidth of 6 RB (i.e. 1.08 MHz) and a maximum of 110 RB (i.e. 19.8 MHz). The basic time unit specified in LTE is $T_s = 1/(F_{sc} \cdot 2048)$, which results on a sampling frequency F_s equal to 30.72 MHz.

LTE signals are constituted by synchronisation signals, reference signals, data signals and control signals. The synchronisation signals and the reference signals are pilot signals (i.e. signals completely known), thus they will be of main interest for positioning. The transmission of transport and control data is not allowed in the synchronisation symbols, neither in the DC subcarrier. Further information on the data-transport channels (i.e. PBCH and PDSCH) and data-control channels (i.e. PDCCH, PCFICH and PHICH) can be found in Ref. 12.

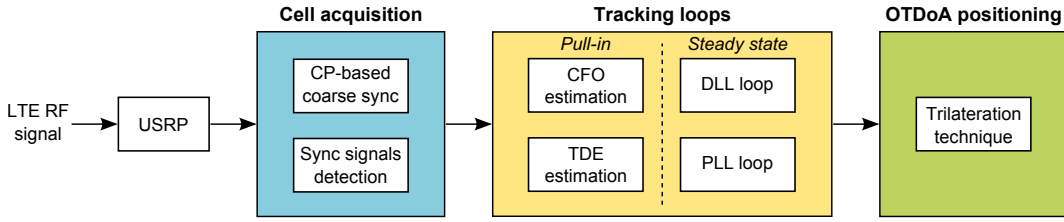


Figure 2. SDR LTE positioning receiver top-level block diagram.

II.A. Synchronisation signals

The synchronization signals are used for cell search and acquisition of the received signal without requiring any assistance data. LTE networks admit up to 504 unique cell identities N_{ID}^{cell} grouped into 168 groups of three sectors. In order to identify every cell, two synchronization signals are periodically broadcast with a specific code for each cell: the Primary Synchronization Signal (PSS) and the Secondary Synchronization Signal (SSS). They are allocated in the center of the spectrum with 62 contiguous pilot subcarriers (independently of the system bandwidth), and avoiding the DC subcarrier. Three different PSS sequences can be used to indicate the cell identity within the group $N_{ID}^{(2)}$, and are defined by three orthogonal Zadoff-Chu (ZC) codes in the frequency domain. The identity of the group $N_{ID}^{(1)}$ (cell ID group) is distinguished by using one of the 168 different SSS sequences. These sequences are generated by scrambling two length-31 m -sequences (maximal length sequences), which differ between subframe 0 and subframe 5. Once both signals are detected, the cell ID is computed as follows,

$$N_{ID}^{cell} = 3 \cdot N_{ID}^{(1)} + N_{ID}^{(2)}. \quad (2)$$

II.B. Reference signals

Several reference signals are specified in the standard, but we will focus only on the cell-specific reference signal (CRS) and the positioning reference signal. The CRS signals are typically used for downlink channel estimation in order to aid data demodulation, but they can also be used for time and frequency tracking. They are scattered in time and frequency following a lattice grid and spanning the maximum bandwidth of the configuration under use. As well as the other reference signals, the CRS is defined by complex-valued sequences generated with length-31 Gold codes, whose initial value depends on the cell identity and the pilot position in time and frequency.

The PRS signals are pilot signals exclusively dedicated for positioning purposes. They are transmitted in specific subframes, called positioning occasion. Each positioning occasion may include from one to six consecutive positioning subframes with a periodicity of 160, 320, 640 or 1280 subframes (of 1 ms). The PRS can be configured to occupy a lower bandwidth than the system bandwidth, in order to increase the spectral efficiency. However, they should not be mapped in resource elements allocated to PBCH, PSS or SSS signals. In addition, the PRS is defined by a subframe offset to the start of the radio frame, defined by a configuration index I_{PRS} .

In single-frequency networks (SFN), the inter-cell interference among base stations may prevent accurate signal measurements, as it is studied in Ref. 8. Thus, the CRS and PRS introduce a frequency reuse factor of six according to the cell identity, i.e. a shift from one to six subcarriers is applied to their frequency pattern given by $N_{ID}^{cell} \bmod 6$. Moreover, a method called PRS muting is specified to further reduce the inter-cell interference, by muting some of the base stations transmitting the PRS signal.

III. SDR LTE positioning receiver

The software-defined radio LTE positioning receiver is implemented in MATLAB by post-processing the signal captured with a USRP platform. As it is shown in figure 2, the SDR is based on three main modules: cell acquisition, tracking loops and OTDoA positioning.

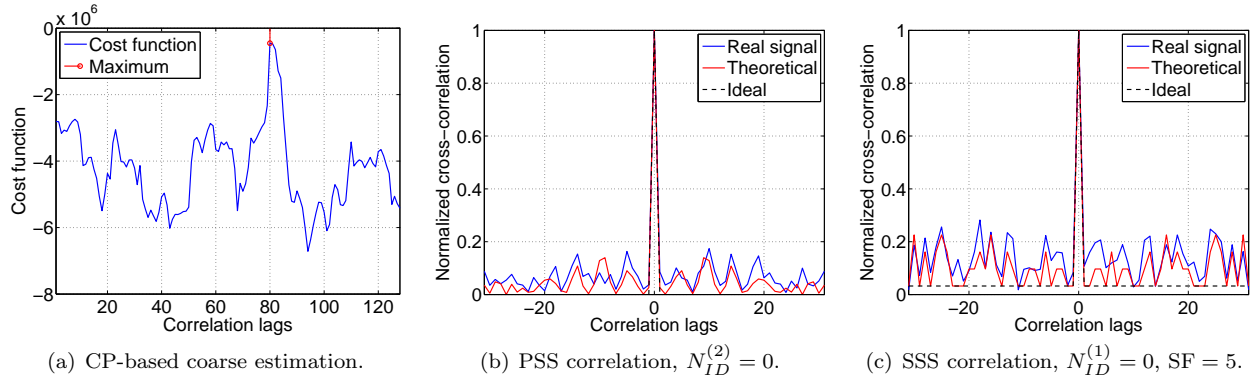


Figure 3. Coarse time and frequency synchronization and cell identity detection.

III.A. Cell acquisition

In any LTE terminal, time and frequency synchronization are of paramount importance for cell acquisition. Generally, frequency synchronization has attracted more attention due to the sensitivity of OFDM receivers to carrier frequency offsets (CFO), but timing errors still have to be compensated in order to avoid severe performance degradation.¹³ Thus, the acquisition stage is based on the coarse time and frequency synchronization and the cell search procedure.

First, the start of the cyclic prefix is found by using the classical van de Beek algorithm,¹⁴ which is a non-data-aided (NDA) maximum likelihood (ML) estimator written as

$$\hat{\tau}_0 = \arg \max_{\tau} \{ |\gamma(\tau)| - \rho \Phi(\tau) \}, \quad (3)$$

with

$$\gamma(k) \doteq \sum_{m=k}^{k+L-1} x(m) \cdot x^*(m+N), \quad (4)$$

$$\Phi(k) \doteq \frac{1}{2} \sum_{m=k}^{k+L-1} |x(m)|^2 + |x(m+N)|^2, \quad (5)$$

where $x(k)$ represents the discrete-time signal samples, m is the correlation lag, L is the normal CP length in samples, and ρ is the correlation coefficient, which is approximated to one for high signal-to-noise ratio (SNR). As it can be noticed, the algorithm takes advantage of the redundancy introduced by the cyclic prefix to coarsely estimate the time delay, using the autocorrelation function $\gamma(k)$, the energy $\Phi(k)$ and a sliding window size of L samples. The complexity of the algorithm can be reduced with a recursive computation of $\gamma(k)$ and $\Phi(k)$.¹⁵ In addition, this estimation can be slightly refined by integrating several times the cost function of Eq. (3). An example of this cost function is shown in figure 3(a). Then, the frequency offset can be coarsely estimated as

$$\hat{\nu}_0 = -\frac{1}{2\pi T} \arg \{ \gamma(\hat{\tau}_0) \}. \quad (6)$$

Given the CP-based estimates $\hat{\tau}_0$ and $\hat{\nu}_0$, the coarse synchronization is completed by compensating these time and frequency shifts on the received signal. Now, the cell detection procedure can be started by removing the cyclic prefix and analysing the signal in the frequency domain. For this purpose, a fast Fourier transform (FFT) is applied to the OFDM signal as

$$r(n) = \mathcal{F} \left\{ x(k + \hat{\tau}_0) \cdot \exp \left(-j \frac{2\pi k \hat{\nu}_0}{N} \right) \right\}, \quad (7)$$

where $\mathcal{F}\{\cdot\}$ is the discrete-time Fourier transform operator. Then, the received frequency symbols $r(n)$ are cross-correlated with the PSS and SSS sequences in order to find the cell identity N_{ID}^{cell} . The applied circular cross-correlation can be expressed as

$$R_u(m) \doteq \sum_{n=-31, n \neq 0}^{31} r^*(n) \cdot d_u(n+m), \quad (8)$$

where $d(n)$ is a circular shifted version of the original pilot sequence and the subscript u denotes the synchronisation sequence (i.e. PSS or SSS). The normalized cross-correlation of the PSS and SSS sequences is shown in figure 3(b) and 3(c), respectively. As it can be noticed, the avoidance on the transmission of the DC subcarrier degrades the code properties of these sequences, where the ideal autocorrelation for the ZC codes is

$$R_{ZC}(m) = \begin{cases} 1 & \text{if } m = 0, \\ 0 & \text{otherwise,} \end{cases} \quad (9)$$

and for the m -sequences is

$$R_M(m) = \begin{cases} 1 & \text{if } m = 0, \\ -1/M & \text{otherwise,} \end{cases} \quad (10)$$

being m the correlation lag, and M equal to 31. Finally, the peak of the correlation leads to the cell identity detection, as follows,

$$\hat{N}_{ID}^{cell} = 3 \cdot \arg \max_{N_{ID}^{(1)}} \left\{ \left| R_{\hat{N}_{ID}^{(1)}}(k) \right| \right\} + \arg \max_{N_{ID}^{(2)}} \left\{ \left| R_{\hat{N}_{ID}^{(2)}}(k) \right| \right\}. \quad (11)$$

where $\hat{N}_{ID}^{(1)}$ and $\hat{N}_{ID}^{(2)}$ are the detected cell identity group and sector, respectively.

III.B. Tracking loops

The residual errors resulting from the coarse synchronisation can severely degrade the time delay estimation. Thus, a pull-in process is implemented in order to further reduce the acquisition errors. This process is based on integrating the outputs of a time delay estimator and a carrier frequency offset estimator among several pilot symbols, to reduce the initial acquisition offsets. Taking advantage of the time shift property of the Fourier transform, i.e. $\mathcal{F}\{x(k \pm \tau)\} = r(n) \cdot \exp(\pm j \frac{2\pi n \tau}{N})$, the TDE estimation becomes a frequency-like estimation problem, and well-known frequency estimators can be adopted for time delay estimation after the FFT operation. For instance, the Fitz estimator proposed in Ref. 16 can be used, as suggested in Ref. 8. Let us describe the modified autocorrelation function as

$$R(m) = \sum_{n \in \mathcal{N}_p} y(n) \cdot y^*(n - m), \quad (12)$$

where the subset of available pilot subcarriers for correlation lag m is expressed as \mathcal{N}_p , and $y(n)$ denotes the OFDM signal after the wipe-off of the pilot code $d(n)$ in the frequency domain, i.e. $y(n) = r(n) \cdot d^*(n)$. Then, the Fitz estimator for time delay estimation of LTE pilot signals can be expressed as⁸

$$\hat{\tau} = \frac{T}{2\pi} \cdot \frac{\sum_{m \in \mathcal{N}_m} \arg\{R(m)\}}{\sum_{m \in \mathcal{N}_m} m}, \quad (13)$$

where \mathcal{N}_m is the subset of available correlation lags. Similarly, a CFO estimator is based on the phase difference between OFDM pilot symbols,¹⁷ which is defined as

$$\hat{\nu} = \frac{N}{2\pi \cdot T \cdot (N + L) \cdot P} \cdot \arg \left\{ \sum_{n \in \mathcal{N}_p} y_{k-P}^*(n) \cdot y_k(n) \right\}, \quad (14)$$

where k is the symbol index and P is the index difference to the previous pilot symbol. Both time and frequency estimators are unbiased for those initial acquisition offsets that fulfil $|\tau| \leq T/2$ and $|\nu| \leq 1/(2T)$, respectively. In order to further reduce the noise effect, several $\hat{\tau}$ and $\hat{\nu}$ estimates are averaged, and the resulting values are used to compensate most of the residual time and frequency errors.

Once the initial offsets are sufficiently reduced, tracking loops are implemented to filter the time delay and frequency estimates. The tracking architecture is based on a first-order delay lock loop (DLL) with a

second-order phase lock loop (PLL) assist.^{18,19} The TDE estimation of Eq. (13) is fed into the DLL. In addition, it is used to compensate the time delay offset and estimate the phase of the pilot subcarriers,

$$\hat{\phi} = \frac{1}{2\pi} \cdot \arg \left\{ \frac{1}{N_p} \sum_{n \in \mathcal{N}_p} y(n) \cdot \exp \left(j \frac{2\pi \cdot n \cdot \hat{\tau}}{N} \right) \right\}, \quad (15)$$

where N_p is the number of pilot subcarriers. Then, the phase estimate $\hat{\phi}$ is introduced in the PLL.

The DLL and PLL loop filter coefficients of first and second order, i.e. c_1 and c_2 , respectively, are calculated according to Ref. 18 as

$$c_1 = \frac{1}{K_0 K_d} \cdot \frac{8\zeta\omega_n T_L}{4 + \zeta\omega_n T_L + (\omega_n T_L)^2}, \quad (16)$$

$$c_2 = \frac{1}{K_0 K_d} \cdot \frac{4(\omega_n T_L)^2}{4 + \zeta\omega_n T_L + (\omega_n T_L)^2}, \quad (17)$$

where $K_0 K_d$ is the loop gain, ζ is the damping ratio, ω_n is the natural frequency, and T_L is the sampling period of the loop. Typical values of the loop design are a loop gain $K_0 K_d$ equal to one and a damping ratio ζ equal to $\sqrt{2}/2$. Given this damping ratio, the natural frequency for the first order filter is $\omega_n = 4B_L$ and for the second order filter is $\omega_n = 1.89B_L$, where B_L is the noise bandwidth in the loop.¹⁹ The frequency shift estimated by the PLL is used to aid the DLL, with the following scale factor $\alpha = F_s/F_c$,¹⁹ where F_c is the carrier center frequency. Finally, the output of the loop filters is integrated in order to track the signal in the next interval.

III.C. OTDoA positioning

Once the receiver is in steady state tracking, its location can be finally calculated by means of the OTDoA positioning method.² This method is based on the time delay differences between the reference BS and the neighbour BSs to compute the position. As it is shown in figure 4, the time-difference measurements follow different hyperbolas that intersect in the receiver or user equipment (UE) location, which is then calculated with a trilateration technique. Taking as a reference the serving BS, i.e. BS 1, the difference between TDE estimates (in seconds) of BS 1 and BS i is defined by a nonlinear equation as²⁰

$$t_1 - t_i = \frac{\sqrt{(x_1 - x)^2 + (y_1 - y)^2} - \sqrt{(x_i - x)^2 + (y_i - y)^2}}{c}, \quad (18)$$

where x and y are the user position coordinates, x_1 and y_1 are the BS 1 coordinates, x_i and y_i are the BS i coordinates, and c is the speed of light. As it can be noticed, the user position unknowns x and y can be solved with at least two time-difference measurements. This computation only requires the knowledge of the base station locations and the time delay offset between their transmission. But in LTE, this information is not provided to the UE. Thus, the UE sends the time-difference measurements, i.e. reference signal time difference (RSTD) measurements, to the network location server, i.e. Evolved Serving Mobile Location Centre (E-SMLC), to estimate the position. Once the position estimate is available, it is then sent back to the user. Although OTDoA is implemented in LTE as a network-based positioning technology, the base stations coordinates and their relative downlink timing are assisted to the SDR receiver in this paper, allowing the UE-based position calculation. The trilateration technique used in the positioning module is based on Fletcher's version of the Levenberg-Marquardt algorithm for minimization of a sum of squares of equation residuals,²¹ which is implemented in a MATLAB function of the MathWorks File Exchange repository.²²

IV. Validation results

The validation of the SDR LTE positioning receiver is performed with a static LTE scenario. The user equipment and the base stations are fixed at specific positions in order to determine the time delay and power received for each signal. Then, a preliminary performance analysis is provided with the SDR position estimates.

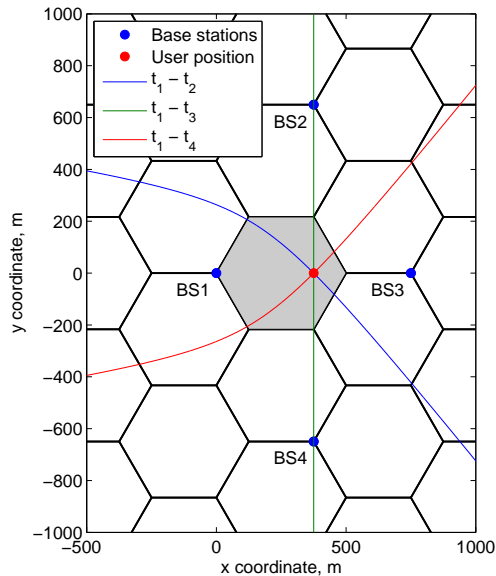


Figure 4. Example of hyperbolas obtained from the time-difference measurements, showing the possible locations of the user and its true position on the intersection of hyperbolas. The base station positions (blue dots) and user position (red dot) are used to define the validation scenario.

IV.A. Scenario definition

The setup of the validation scenario is based on a LTE network emulator, the USRP platform and the SDR positioning receiver. The LTE network is emulated using two Spirent E2010S network emulators of the European Navigation Laboratory (ENL) at the European Space Agency (ESTEC, The Netherlands). These two emulators generate four synchronized LTE signals, each signal corresponding to a base station. The four BSs are assumed to belong to the same network operator, thus they are transmitting in the same frequency channel, leading to intra-frequency RSTD measurements. The band 3 at 1800 MHz is chosen for the downlink signal transmission, because it is the most popular spectrum for LTE commercial deployments.⁴ Particularly, the E-UTRA Absolute Radio Frequency Channel Number (EARFCN)²³ is the 1750, corresponding to a carrier center frequency of 1860 MHz.

The physical layer of the network emulator is configured with a system bandwidth of 1.4 MHz. The PRS signal is transmitted in the whole bandwidth every 160 ms for six consecutive subframes and an offset of two subframes (i.e. $I_{PRS} = 2$). In addition, the network emulator requires as inputs the received power and time delay for each BS. Thus, an urban macro-cell deployment is simulated with a inter-site distance (ISD) of 750 meters, as in Ref. 8 and 9. The deployment is based on a hexagonal grid with three-sectorial base stations (i.e. 3 dB-beamwidth of 65-degree). As in figure 4, the UE is located at coordinates $\{x, y\} = \{\text{ISD}/2, 0\}$ in meters, and the BSs are at coordinates $\{x_i, y_i\} = \text{ISD}/2 \cdot \{0, 0; 1, \sqrt{3}; 2, 0; 1, -\sqrt{3}\}$ also in meters. Considering the parameters summarized in Table 1, the received signal power from BS i is computed using the expression given in Ref. 24,

$$P_{rx,i} = P_{tx,i} - \max(L_i - G_{tx,i} - G_{rx}, \text{MCL}), \quad (19)$$

where $P_{tx,i}$ is the transmitted signal power, L_i is the macroscopic pathloss, $G_{tx,i}$ is the transmitter antenna gain, G_{rx} is the receiver antenna gain and MCL is the minimum coupling loss,²⁴ defined as the minimum path loss between mobile and base station antenna connectors. The resulting received power values are: $P_{rx,i} = \{-54.08, -65.61, -64.31, -65.61\}$ in dBm. Similar power budget calculations can be found implemented in MATLAB-based simulators.²⁵ The potential inter-cell interference produced by the deployment of more base stations will not be considered. The application of shadowing or multipath are out of the scope of this study.

Once the network emulators are configured, their RF outputs are combined and fed to a USRP N210 platform installed with a DBSRX2 daughterboard. The USRP is then connected through the Gigabit Ethernet port and controlled with the USRP hardware driver (UHD) from a computer. The UHD commands the recording of the complex baseband samples at a sampling ratio of 2 MHz. Finally, the samples are loaded with MATLAB and downsampled to 1.92 MHz, where the LTE signals are processed with the SDR receiver described in Section III. The SDR receiver is assisted with the cell identities and relative time delays of

Table 1. Base station simulation parameters according to Ref. 24.

BS signal power	$P_{tx} = 43$ dBm
BS antenna radiation pattern	$G_{tx} = \bar{G}_{tx} - \min \{ 12 \cdot (\theta/\theta_{3dB})^2, A_m \}$
BS antenna mean gain	$\bar{G}_{tx} = 15$ dBi
BS antenna model	3 dB beam width, $\theta_{3dB} = 65$ degrees
BS antenna minimum attenuation	$A_m = 20$ dB
Minimum coupling loss	MCL = 70 dB
Path loss model ¹	$L_i = 128.1 + 37.6 \log_{10}(R_i)$ dB
UE antenna model	Omnidirectional, $G_{rx} = 0$ dBi

¹ R_i is the propagation distance to BS i in meters.

the base stations emulated. The serving cell identity (i.e. BS 1) is first acquired and detected. Then, the assistance information is used to avoid the neighbour cell identification. Since the SDR receiver does not communicate with the network, no user data is transmitted by the emulated BSs. Thus, there are cell-specific reference signals without inter-cell interference. These CRS signals are used for tracking purposes and to validate the positioning module in absence of inter-cell interference and multipath, i.e. only in additive white Gaussian noise (AWGN) conditions.

IV.B. Positioning results

The SDR receiver is able to acquire and synchronise the signals of four base stations, leading to an accurate spectrum response, as it is shown in figure 5. Observing the CRS and PRS signals, they are shifted in frequency according to the specific cell identities. As expected, the serving cell (i.e. BS 1) has a higher power than the neighbour cells.

After the acquisition and the pull-in process, the DLL and PLL loops track the frequency and the observed time-difference of arrival of the received signals, as it can be seen in figure 6(a) and 6(b). The noise bandwidth B_L of the DLL and PLL is set to 1 Hz and 20 Hz, respectively. Since the CRS symbols without interference are only used for estimation, measurements are taken every slot, thus the sampling period of the loops T_L is equal to 0.5 ms.

The user position is finally estimated using the OTDoA measurements, as it is shown in figure 6(c). The estimated positions are obtained after the calibration of the transmission timing offset between LTE signals of the network emulators. However, there is still a bias on the mean value estimated with respect to the true user position, which is approximately equal to 34 cm. In addition, the standard deviation for x and y coordinates is plotted with an ellipse. As it can be seen, the position errors in the x coordinate are lower than in the y coordinate. This is due to the distribution of the base stations and the user position, depicted in figure 4. The cumulative density function (CDF) of the position errors obtained with the SDR receiver are shown in figure 6(d). As it can be seen, accurate position estimations with errors lower than three meters can be achieved in a static AWGN scenario for a signal bandwidth of 1.08 MHz (i.e. 6 RB).

V. Conclusion

A software-defined radio (SDR) LTE positioning receiver is presented with a detailed description of its architecture. The acquisition and detection of LTE signals corresponding to four different cells is achieved. Frequency and time-delay synchronization is performed in the frequency domain with tracking loops. This synchronisation allows the estimation of three observed time-difference of arrival (OTDoA) in order to compute the position of the user. The receiver positioning module is validated in a static scenario showing a position accuracy lower than three meters in AWGN conditions. Thus, the tool can be an essential element to assess the performance of hybrid GNSS and LTE positioning systems, which could be expanded to any hybrid fusion of satellite and terrestrial signals. Future work is aimed towards this hybrid approach, as well as the performance assessment of LTE achievable positioning capabilities. In addition, the real-time implementation of the receiver may help to test commercial LTE network deployments.

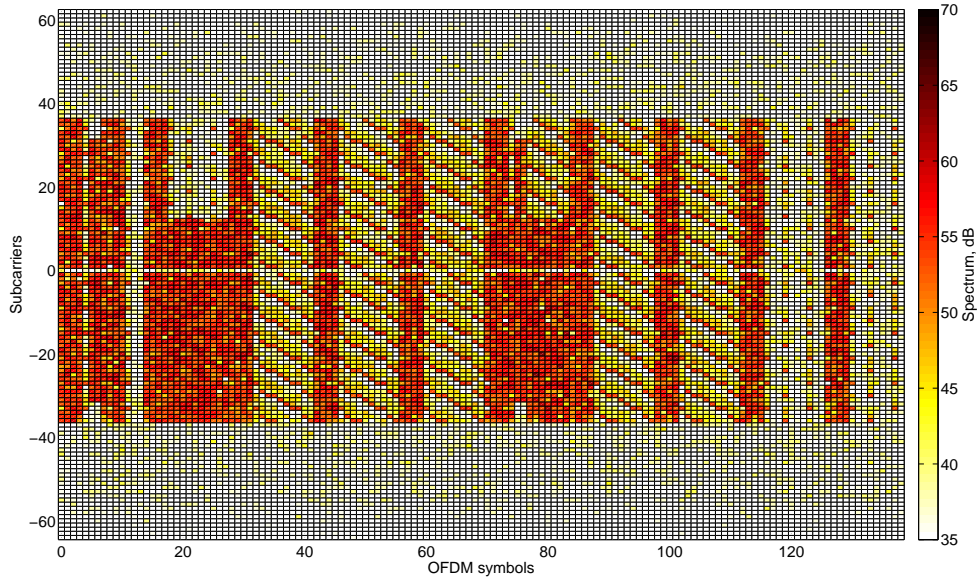
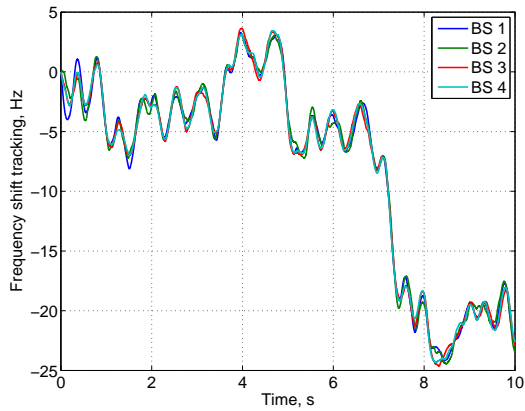
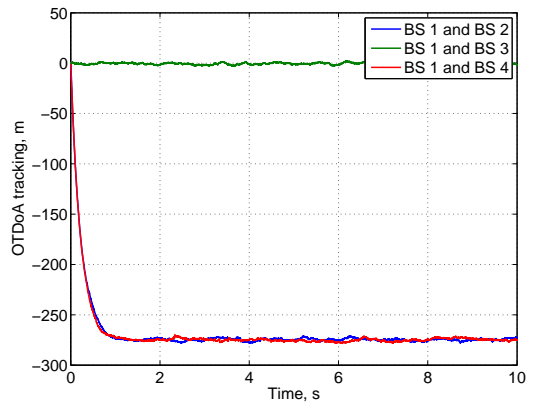


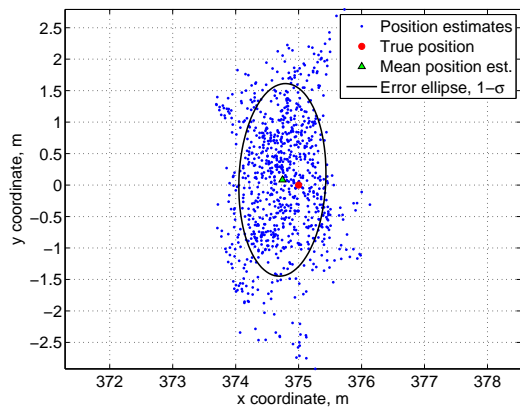
Figure 5. Time and frequency spectrum of a PRS-enabled LTE radio frame for the validation scenario with four base stations.



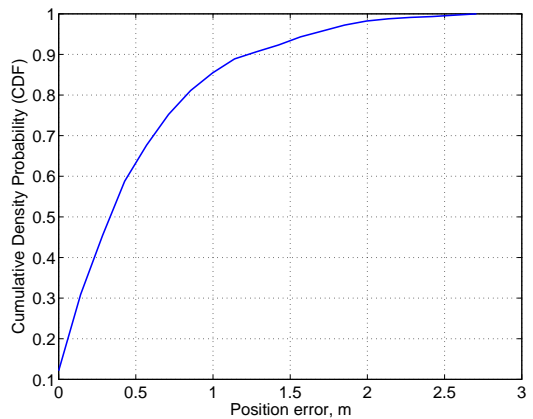
(a) Frequency shift tracked by PLL.



(b) OTDoA tracked by DLL.



(c) Position estimations and true position.



(d) CDF of position errors.

Figure 6. Tracking and positioning results of the SDR LTE receiver for four LTE signals of 1.08 MHz (i.e. 6 RB) bandwidth in a static AWGN scenario.

Acknowledgments

The content of the present article reflects solely the authors view and by no means represents the official ESA view. This work was supported by the ESA under the PRESTIGE programme ESA-P-2010-TEC-ETN-01 and by the Spanish Ministry of Science and Innovation project TEC 2011-28219.

The authors would also like to convey thanks to Moisés Navarro-Gallardo and Juan Manuel Parro-Jiménez from Universitat Autònoma de Barcelona (UAB) for their help on the USRP platform.

References

- ¹3GPP TS 36.211, “Evolved Universal Terrestrial Radio Access (E-UTRA); Physical channels and modulation,” Technical Specification, Rel. 9, 2009.
- ²3GPP TS 36.305, “Evolved Universal Terrestrial Radio Access Network (E-UTRAN); Stage 2 functional specification of User Equipment (UE) positioning in E-UTRAN,” Technical Specification, Rel. 9, 2009.
- ³Van Diggelen, F. S. T., *A-GPS: Assisted GPS, GNSS, and SBAS*, Artech House, 2009.
- ⁴GSA - Global mobile Suppliers Association, “GSA Status of the LTE Ecosystem report: 948 LTE User Devices launched by 100 suppliers,” Tech. rep., July 2013.
- ⁵Working Group 3, E9-1-1 Location Accuracy, “Report – Leveraging LBS and Emerging Location Technologies for Indoor Wireless E9-1-1,” Tech. rep., The Communications Security, Reliability and Interoperability Council III (CSRIC 3), Federal Communications Commission (FCC), March 2013.
- ⁶R1-090353, “On OTDOA in LTE,” 3GPP, Qualcomm Europe, RAN1-55bis, Ljubljana, Slovenia, Jan. 2009.
- ⁷R1-092307, “Analysis of UE subframe timing offset measurement sensitivity to OTDoA performance,” 3GPP, Alcatel-Lucent, RAN1-57bis, Los Angeles, USA, June 2009.
- ⁸Del Peral-Rosado, J. A., López-Salcedo, J. A., Seco-Granados, G., Zanier, F., and Crisci, M., “Achievable Localization Performance Accuracy of the Positioning Reference Signal of 3GPP LTE,” *Proc. ICL-GNSS*, June 2012.
- ⁹Del Peral-Rosado, J. A., López-Salcedo, J. A., Seco-Granados, G., Zanier, F., and Crisci, M., “Analysis of Positioning Capabilities of 3GPP LTE,” *Proc. International Technical Meeting of The Satellite Division of the Institute of Navigation (ION GNSS)*, Sept. 2012, pp. 650–659.
- ¹⁰Medbo, J., Siomina, I., Kangas, A., and Furuskog, J., “Propagation channel impact on LTE positioning accuracy: A study based on real measurements of observed time difference of arrival,” *Proc. IEEE Personal, Indoor and Mobile Radio Communications (PIMRC)*, Sept. 2009, pp. 2213–2217.
- ¹¹Gentner, C., Rawadi, J.-M., Munoz, E., and Khider, M., “Hybrid Positioning with 3GPP-LTE and GPS Employing Particle Filters,” *Proc. International Technical Meeting of The Satellite Division of the Institute of Navigation (ION GNSS)*, Sept. 2012, pp. 473–481.
- ¹²Sesia, S., Toufik, I., and Baker, M., *LTE – The UMTS Long Term Evolution: From Theory to Practice*, John Wiley & Sons, 2011.
- ¹³Morelli, M., Kuo, C.-C., and Pun, M.-O., “Synchronization Techniques for Orthogonal Frequency Division Multiple Access (OFDMA): A Tutorial Review,” *Proceedings of the IEEE*, Vol. 95, No. 7, 2007, pp. 1394–1427.
- ¹⁴van de Beek, J., Sandell, M., and Borjesson, P., “ML estimation of time and frequency offset in OFDM systems,” *IEEE Trans. on Signal Processing*, Vol. 45, No. 7, July 1997, pp. 1800–1805.
- ¹⁵Manolakis, K., Estevez, G., Jungnickel, V., Xu, W., and Drewes, C., “A closed concept for synchronization and cell search in 3GPP LTE systems,” *IEEE Wireless Communications and Networking Conference (WCNC)*, 2009, pp. 1–6.
- ¹⁶Fitz, M., “Planar filtered techniques for burst mode carrier synchronization,” *Proc. IEEE GLOBECOM '91*, Vol. 1, Dec. 1991, pp. 365–369.
- ¹⁷Moose, P. H., “A technique for orthogonal frequency division multiplexing frequency offset correction,” *IEEE Transactions on Communications*, Vol. 42, No. 10, 1994, pp. 2908–2914.
- ¹⁸Borre, K., Akos, D., Bertelsen, N., Rinder, P., and Jensen, S., *A software-defined GPS and Galileo receiver: a single-frequency approach*, Birkhauser, 2007.
- ¹⁹Ward, P. W., Betz, J. W., and Hegarty, C. J., “Satellite Signal Acquisition, Tracking, and Data Demodulation,” *Understanding GPS: Principles and Applications*, edited by E. Kaplan and C. Hegarty, chap. 5, Artech House Publishers, Boston, London, 2nd ed., 2006, pp. 153–241.
- ²⁰Buehrer, R. M. and Venkatesh, S., “Fundamentals of Time-of-Arrival-Based Position Locations,” *Handbook of Position Location: Theory, Practice, and Advances*, edited by S. A. R. Zekavat and R. M. Buehrer, chap. 6, John Wiley & Sons, Inc., 1st ed., 2012, pp. 175–212.
- ²¹Fletcher, R., “A Modified Marquardt Subroutine for Non-linear Least Squares.” Tech. rep., Atomic Energy Research Establishment, Harwell, England, 1971.
- ²²Balda, M., “LMFsolve.m: Levenberg-Marquardt-Fletcher algorithm for nonlinear least squares problems,” MathWorks, File Exchange, ID 16063, 2007.
- ²³3GPP TS 36.104, “Evolved Universal Terrestrial Radio Access (E-UTRA); Base Station (BS) radio transmission and reception,” Technical Specification, Rel. 9, 2009.
- ²⁴3GPP TR 36.942, “Evolved Universal Terrestrial Radio Access (E-UTRA); Radio Frequency (RF) system scenarios,” Technical Specification, Rel. 9, 2009.
- ²⁵Mehlführer, C., Ikuno, J. C. C., Šimko, M., Schwarz, S., Wrulich, M., and Rupp, M., “The Vienna LTE simulators-Enabling reproducibility in wireless communications research,” *EURASIP Journal on Advances in Signal Processing*, Vol. 2011, No. 1, 2011, pp. 1–14.